Optimal Design Of Fused Deposition Modeling Structures Using Comsol Multiphysics

F. Roger* Department of Polymers and Composites Technology & Mechanical Engineering, Mines Douai, 941 rue Charles Bourseul, CS 10838, 59508 Douai, France
*frederic.roger@mines-douai.fr

Abstract: Optimal design and manufacturing of 3d printed mechanical parts can be conducted using Comsol multiphysics©.
In this paper, a strategy combining topological optimization, optimal infill with heterogeneous structures or multi-materials and process modeling is proposed.
This strategy is applied for thermoplastics parts printed by fused filaments or droplets deposition. For multi-materials parts, interfaces weaken the mechanical performances. Interfaces strength and microstructures are analyzed using respectively tensile tests and computed micro-tomography scans for an assembly of ABS and Carbon black filled ABS. Infill patterns at the interface, and printed part orientation on the platform have significant influences on the mechanical resistance. Quality of adhesion between filaments, which can be defined by porosities distributions, and the relative orientation between layers are key factors for fatigue resistance. Modeling heat transfers and varying printing conditions help to compare infill strategies considering the relative temperature between filaments to estimate the quality of adhesion.

Keywords: 3d-printing**,** additive manufacturing topological optimization**,** thermoplastics**,** multi-materials

1. Introduction

Combination of additive manufacturing (AM) and topological optimization offer new opportunities in mechanical design without limitation on structure geometry [1,2]. Fused Deposition Modeling is a widely used Additive Manufacturing process which is affordable with a free control of process parameters. In this paper, we try to improve the design of structures using first topological optimization to define the external geometry and then to use either heterogeneous internal filling or multi-materials. Indeed, based on structural mechanics simulation, parts of the structures with high stresses are printed with high density internal filling or alternatively we add a new material with improved mechanical properties. In our example, two materials are combined: red ABS and black conductive ABS (ABS with carbon black). In our optimization approach, conductive ABS can be replaced with other materials like ABS with reinforced fillers to increase the stiffness. While the optimal inner and outer designs are defined, another challenge is to find the best manufacturing parameters. During the 3d printed of variable densities filled parts or multi-materials parts, weak interfaces are created. The mechanical strength of these interfaces is strongly linked to the printing patterns. In addition to tensile tests, computed micro-tomography analysis gives 3D description of microstructures and highlights the spatial distribution of voids that governs mechanical and fatigue strengths of parts. Good adhesion between filaments is related to local temperature and relative temperature between side by side filaments during deposition. Modeling heat and mass transfers during 3d printing permits to estimate this temperature parameters and then to compare patterns depositions strategies.

2. Topological optimization of outer geometry of part

2.1 Part configuration and governing equations

A symmetrical mechanical structure submitted to tensile loading is considered. The figure 1 shows the initial geometry and the corresponding boundary conditions. The combined topological optimization and structural mechanics simulations are performed using Comsol multiphysics. The goal of the optimization is to minimize the total weight with a distribution of materials that maximize the stiffness. The upper bound of the new surface area must be less than 50% of the initial surface area.

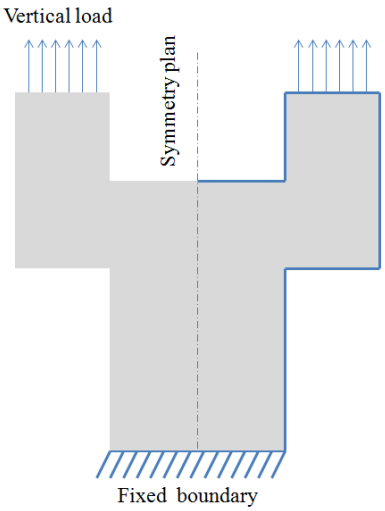

Figure 1. - Initial geometry and boundary conditions for the topological optimization

The Solid Isotropic Material with Penalization method (SIMP) [3,4] is used to minimize the total strain energy W_s or maximize the stiffness for a fixed amount of material. The control variable is the artificial density ρ_{design}. Local Young's modulus is a function of the initial Young modulus E_0 and is defined by the following equation:

$$E(x) = \rho_{design}\,(x)^p E_0$$

The exponent p (p=5) is added in order to discourage the formation of intermediate density. The density parameter is constrained such that $10^{-9} \leq \rho^p \leq 1$. The small lower bound is used for numerical reasons. During the optimization process, the fraction of material used by the new structure is bounded by the following integral inequality constraint:

$$0 \leq \int_{\Omega} \rho_{design}\,(x) d\Omega \leq 0.5A$$

Where A is the initial surface area. Minimizing the total strain energy while limiting the variation of density in the computational domain is realized minimizing the following objective function:

$$f=\frac{(1-q)}{Ws_0}\int_{\Omega} W_s(x)d\Omega + q\,\frac{h_0 h_{max}}{A}\int_{\Omega} \left|\nabla \rho_{design}\,(x)\right|^2 d\Omega$$

where q is a parameter that controls the fraction (1-q) of objective term (first term) and the fraction q of the penalty term (second term). Ws_0 is the total strain energy stored by the non-optimized structure for a constant fraction ρ_{design} set to 0.5 in the whole domain. h_0 and h_{max} are respectively the initial mesh size and the current mesh size. The first integral term of equation corresponds to the minimization of the normalized total strain energy. The last integral term is added to penalize the total variation of the design variable.

2.2 Optimal outer geometry and corresponding stresses distribution

The figure 2 shows the distribution of Young's modulus after optimization which defines the optimal geometry by color contrast (a) and the corresponding Von Mises stresses fields evaluated on a optimal cleaned structure (b). Cleaning procedure consists in making binary image of figure 2a, detecting edges and extracting points coordinates using ImageJ free software. After curves interpolations, a 2D-3D STL conversion by shape extrusion is performed using Comsol Multiphysics.

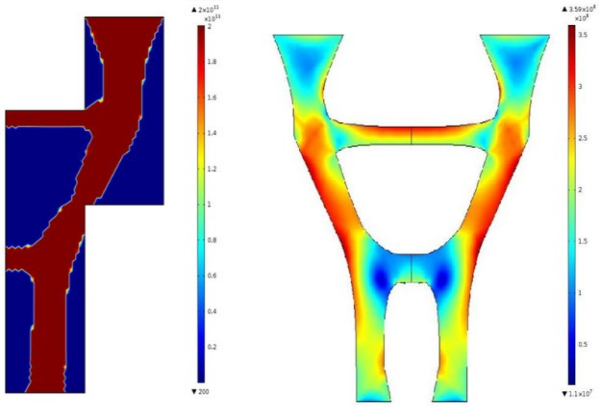

(a) (b)

Figure 2. - Young's modulus (Pa) distribution defining the optimal shape (brown domain) (a) and stresses field (Pa) in the cleaned geometry (b).

The figure 2b shows the stresses distribution in the optimal structure extracted from the topological optimization simulation after cleaning. Stress level is particularly high in the middle height of the part. The next step is to manufacture the structure by fused deposition modeling considering firstly a heterogeneous filling and secondly the use of multi-materials. The goal is to apply specific manufacturing conditions in the critical zones of the structure corresponding to high mechanical stresses.

In order to apply a specific manufacturing treatment in the mid-height of the part, the structure is divided into three domains as defined by figure 3. This choice is based on stresses concentration field (Fig2b) to include high stresses domains in a high performance material domain.

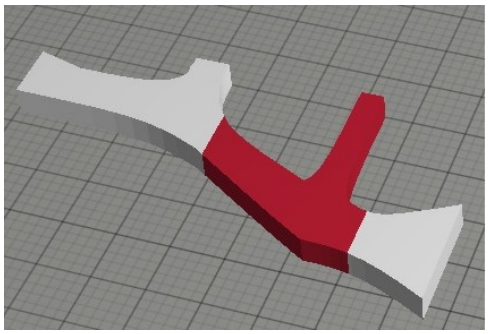

Figure 3. - Splitting of the optimal geometry to apply a specific manufacturing treatment in the middle zone

3. Optimal infill strategy

3.1 Heterogeneous infill

The FDM additive manufacturing process makes it possible to control the internal structure of the 3D-printed object. Indeed, the slicer software proposes settings to control the fraction of material and the infill pattern geometry. Infill optimization is another way to reduce weight while maintaining good mechanical performances. For example, it is well known that honeycomb shapes provide a high resistance in compression with a high fraction of voids and are thus used for load-bearing structures.
Rectilinear patterns are used for the different parts of the structure with a fraction of 20% of material for the external parts (grey zones in figure 3) and a fraction of 60% of material for the mid-height part (red zone in figure 3). The corresponding fractions are selected to create a more resistant domain in the high stresses concentration domain (middle part) while maintaining a lightweight structure.
The elementary cell has a squared shape which is appropriated for tensile loading conditions. The figure 4 shows the 3D-printed structure with the corresponding infill. Virgin ABS material colored in red is used in this case.

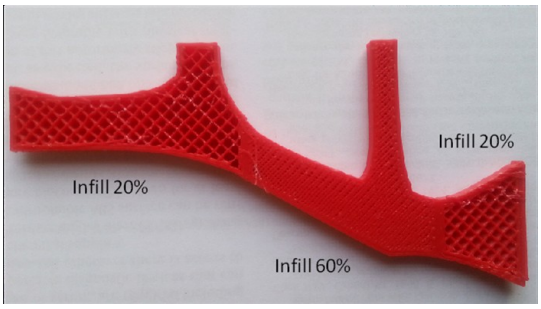

Figure 4. - Inner rectilinear filling of the optimized structure with variable densities

The infill angles are 45 and -45° related to the height direction. The increasing of infill density is an efficient way to improve stiffness.

3.2. Use of several materials

Some FDM 3D-printers are equipped with multiple extruders, making it possible to produce multi-materials manufactured objects. Multi-materials can be the association of different thermoplastics or of a given thermoplastic and its filled/reinforced counterpart. Multi-materials can be used to improve flexibility or to increase the stiffness in specific parts. Conductive polymers can be used to convey electricity in the core or the surface of the object or to attenuate electromagnetic interference emissions [5].
In the present case study, the critical part for the structure (mid-height part) is made of carbon black-filled ABS while keeping virgin ABS elsewhere. Addition of fillers results in a conductive polymer by percolation. The conductive polymer can be easily replaced by stiff particles-filled polymers to improve the stiffness.

Figure 5. - Optimized structure printed with two different materials

3.3 Assessment of interface properties

Finding the optimal conditions for good adhesion between the different polymers used is a challenge. First of all compatibility between polymers is of course required. Considering the printing process, the polymer thread temperature at each side of the interface must be close to the melting temperature. Printing of threads at each side of the interface must be consecutive to insure these temperature conditions.

To find the best conditions for 3d printing of multimaterials with good resistance at the interfaces, we have printed three bi-materials samples with various process conditions and have submitted them to tensile tests. The samples are shown in figure 6.

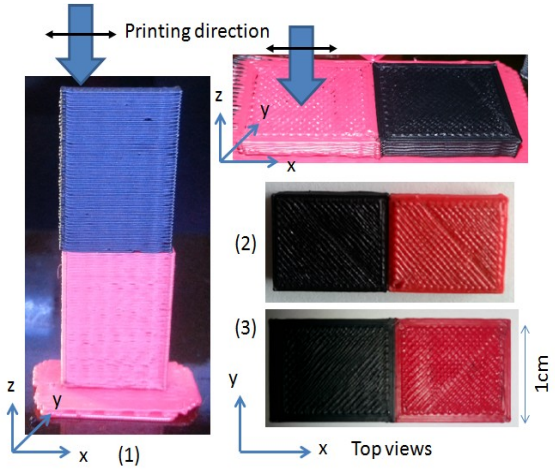

Figure 6. - Bimaterials samples : (1) vertical printing, (2) horizontal printing with side by side parts, (3) horizontal printing with side by side and interpenetrated layers at the interface.

The first sample has been printed in vertical position (vertical stacking of layers) where the interface layers are printed consecutively. We expect that in this configuration the interface resistance will be optimal.

The second sample has been printed in horizontal position with two parts placed side by side without gap between them. Unfortunately the quality of the interface is very brittle and macro-cracks appear after printing.

For the third sample, to improve the adhesion between layers at the interface, we propose a horizontal printing configuration but with alternative interpenetration of each material layer on a short distance at the interface. In horizontal position, filaments on each side of the interface are printed in the same direction parallel to the interface.

As the sample 2 interface is damaged after printing, tensile tests are only conducted for bi-materials samples 1 and 3, loaded in z and x directions respectively. Ultimate tensile stresses are respectively 3.2 and 6.24 MPa.

Tensile tests are also conducted for each ABS material on 3d printed samples and gives 10.55Mpa for carbon black filled ABS and 23MPa for red ABS. These results show that multimaterials interface weaken the mechanical performance of 3d printed objects. However, an optimal stacking strategy with interpenetration of layers at the interface can clearly improve the ultimate tensile strength. In our case, ultimate tensile strength is twice for sample 3 compared to sample 1.

X-Ray Computed tomography analysis is conducted for each interface with a voxel size of 5µm. The figure 7 shows the voids distribution at the interface of sample 1 and 3 after image processing using the free ImageJ software.

For sample 1, the large voids are related to variation of infill layers orientation during deposition. This is the origin of the premature rupture during tensile test. The sample 3 with interpenetration of filaments at the interface shows smaller voids and several zones of continuity along the whole width of the specimen leading to an improved resistance.

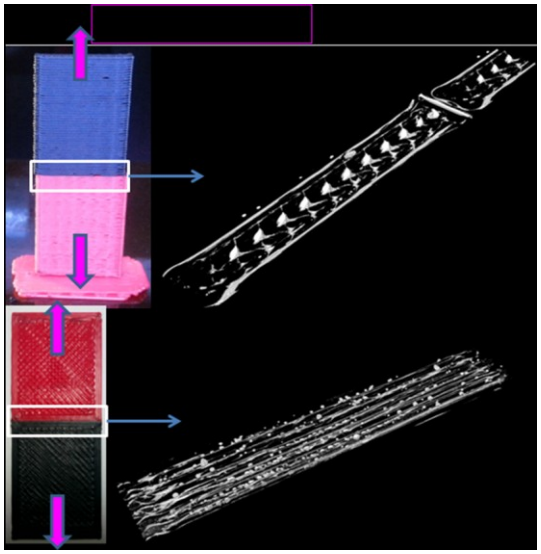

Figure 7. – Voids distribution at the interface for samples 1 and 3 (from Computed micro-tomography) and tensile test directions.

4. Heat and mass transfer modeling of fused thermoplastics deposition

Multiphysics modeling of fused thermoplastics deposition can help to predict thermal history, wetting conditions, possible polymer crystallization and residual stresses and strains.
The biggest challenge is to model the material deposition with interactions between filaments.
In this part, we focus on heat transfer as the first step of thermomechanical modeling. Infrared thermography is used to evaluate cooling rate and to adjust heat sources corresponding to hot material deposition.

4.1 heat transfer in a plate

This part corresponds to the simulation of the first layer filling of a squared plate made with PLA. Material addition is not considered in this example. A surface heat source is moving along the deposition patterns at the extruder scanning speed and convective heat transfer coefficient is adjusted according to infrared thermography analysis. The figure 8 shows the measured temperature distribution during the printing. Temperatures vary from room temperature to 190°C which is the PLA temperature at the end of the extruder. Cooling rate of 80°/s is extracted from IR monitoring.

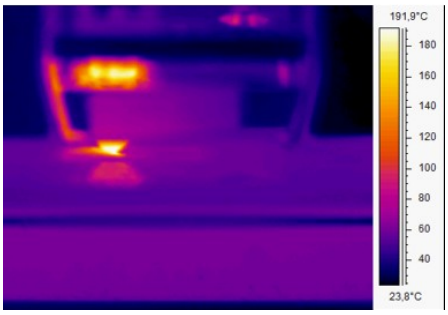

Figure 8. – Temperature distribution during FDM of PLA extracted using infrared thermography.

The figure 9 shows the temperature field during infill simulation of the plate.

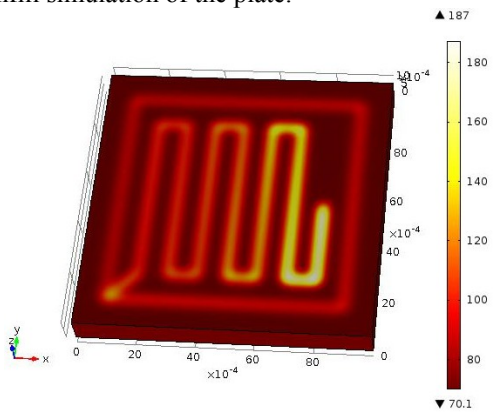

Figure 9. – Temperature distribution during FDM simulation of PLA**.**

If we apply a post-processing filter where zones of temperature above 140°C are highlights, we can monitor the zone of possible coalescence between filaments. This limit has been arbitrary selected and can be adjusted. Figure 10 shows such a post-processing which can be applied during the whole printing process.

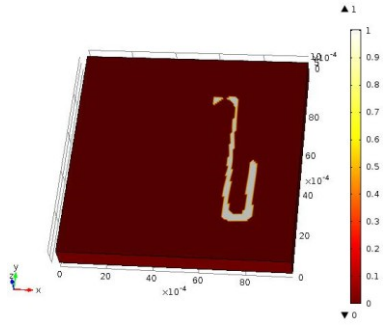

Figure 10. – Temperature distribution above 140°C at the same time step as figure 9 during FDM simulation of PLA **.**

4.2. Heat and mass transfer in a thin walled tube

This simulation corresponds to heat and mass transfer in the first two layers of a thin walled tube (outer diameter 10mm) and has been developed to model high frequency (60-200Hz) plastic droplets (diameter 180 to 300µm) deposition process which is a additive manufacturing process named Freeformer developed by Arburg© company [6]. At highest frequencies, droplets deposition leads to continuous filament and the process is similar to Fused Deposition Modeling. However, in the case of freeformer, the 3d-printing takes place in a temperature controlled closed chamber able to cover 50-120°C. In the simulation the droplet diameter is set to 200 µm, the first layer scanning speed (40mm/s) is reduced to half of the second one to improve adhesion on the platform.

To model the material deposition, the whole extruder path domain is pre-meshed and meshes are activated continuously according to the current position of the extruder. An Ordinary Differential Equation is added to heat transfer model, its variable defines the mesh elements which are thermally activated. A volumetric heat source is moving along the deposition pattern and heats the filament up to fusion temperature (230°C for ABS droplets). The temperature of printing chamber is set to 80°C.

The figure 11 shows finite elements that are activated (a) and the corresponding thermal field during the deposition of the second layers (b).

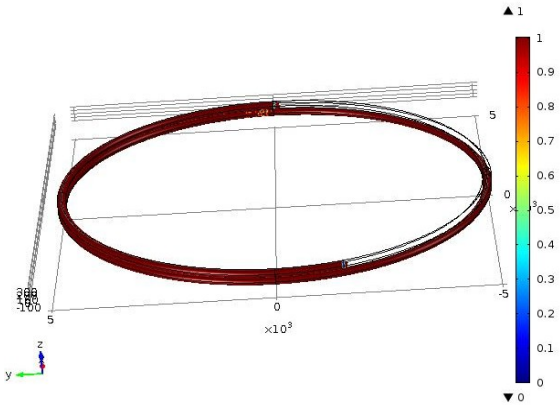

(a)

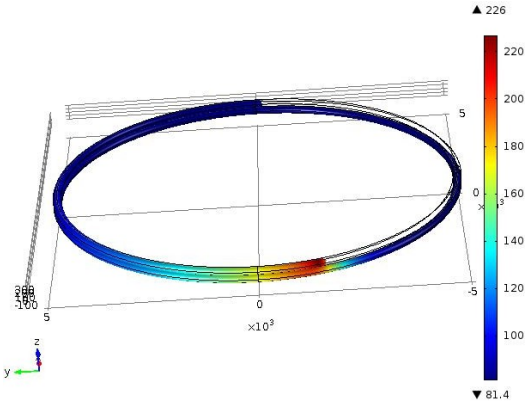

(b)

Figure 11. – (a) activated elements at t=1s and (b) corresponding temperature field (°C)

Combining heat transfer model and mesh element activation permits to simulate transient temperature field between filaments and to compare several 3d printing conditions to find the best manufacturing strategy.

5. Conclusion

A three steps strategy has been developed to optimize 3d printing parts geometry and the infill conditions. Topological optimization with Comsol Multiphysics using "Solid Isotropic Material with Penalization" leads to optimal outer shape of the part. For the infill, we propose two approaches: either to use heterogeneous infill with variable filling density in the part or to use several materials. Higher density infill or more resistant material are placed in the high stresses zones of the part. In the case of multimaterials, interfaces are the weakest zones. Using interpenetration of layers at the interface can improve significantly the mechanical resistance.

Finally, heat and mass transfer models during fused filament or droplets deposition are proposed. Adjusting heat sources and heat convection conditions can lead to a predictive simulation of thermal history during 3d printing. This is the first step of the thermomechanical modeling of 3d printing processes based on fused thermoplastics deposition.

6. References

1. R. Rezaie, M. Badrossamay, A. Ghaie, H. Moosavi, Topology Optimization for Fused Deposition Modeling Process**,** *Procedia CIRP***, Volume 6**, pp 521-526 (2013)

2. F. Roger, P. Krawczak, 3D-printing of thermoplastic structures by FDM using heterogeneous infill and multi-materials: An integrated design-advanced manufacturing approach for factories of the future, *Congrès Français de Mécanique*, Lyon, 24-28 aout 2015.

3. M.P Bendsoe, *Optimal shape design as a material distribution problem*, Structural Optimization, **Volume 1**, page 193-202 (1989)

4. Introduction to the Optimization Module, Topology Optimization of an MBB Beam. *Comsol Multiphysics documentation.*

5. J.M. Thomassin, C. Jérôme, T. Pardoen, C. Bailly, I. Huynen, C. Detrembleur, Polymer/carbon based composites as electromagnetic interference (EMI) shielding materials**,** *Materials Science and Engineering*, **Volume 74**, Issue 7, pp 211-232 (2013)

6. M. Neff, O. Kessling, Layered Functional Parts on an Industrial Scale**,** *Kunststoffe international*, **Volume 8**, pp 40-43 (2014)

7. Acknowledgements

The author gratefully acknowledges the International Campus on Safety and Intermodality in Transportation (CISIT), France, the Nord-Pas-de-Calais Region and the European Community (FEDER funds) for partly funding the X-ray tomography equipment.
The author also acknowledges, Lahcène Cherfa, Unité de Mécanique, ENSTA Paristech, France for its collaboration on the infrared thermography analysis.